submitted to Journal of Nonlinear Optical Physics & Materials

# Nonlinear Absorption in Phthalocyanine Thin Films and Solutions Using a Continuous Wave Laser

Nathaniel Morrison, Thomas Gredig

Department of Physics and Astronomy, California State University, Long Beach, CA
90840-9505, USA.
tgredig@csulb.edu

Received Nov 2, 2021

The nonlinear absorption of nanoscale thin films of iron phthalocyanine, zinc phthalocyanine, and metal-free phthalocyanine fabricated via thermal evaporation at various deposition temperatures was studied using the open-aperture z-scan method with a continuous wave laser. A solution of tetra-tert-butyl-phthalocyanine in chloroform was also studied via z-scan. The thin films exhibit pronounced saturable absorption, with the degree of nonlinearity highly dependent on the type of metal complex. No significant correlation was found between deposition temperature and nonlinear absorption. The liquid sample exhibits a transition from saturable absorption to reverse saturable absorption at high irradiance.

Keywords: phthalocyanine; nonlinear absorption; z-scan

# 1. Introduction

The proliferation of lasers in industrial, commercial, military, and scientific applications has heightened the need for improved laser safety lenses for optical sensors and the human eye. Optical limiters are promising candidates for next generation safety lenses, allowing for greater transparency under normal conditions while providing protection equivalent to current materials. The field of nonlinear optical properties in phthalocyanine-related molecules has been developed over the last three decades 15. Phthalocyanine (Pc) and its derivatives have been widely studied as optical limiter candidates, and have shown considerable promise<sup>3,5,8,11,19,21,23,24,25,27,31</sup>. This molecular family is particularly suitable towards nonlinear optical properties as it has many delocalized  $\pi$ -electrons<sup>8</sup>. Outstanding questions include the effect of crystal size<sup>10,20</sup>. When exposed to a pulsed laser, Pc acts as a strong reverse saturable absorber (RSA), a material in which the excited state absorption cross section is greater than the ground state cross section. At high fluences, a greater portion of molecules become excited, increasing absorption - an optical limiter. In Pc, it is thought that this is primarily due to two-photon absorption<sup>3,5,27</sup>, although other nonlinear processes such as three-photon absorption<sup>22</sup> have also been suggested as contributors.

Beyond its high degree of optical nonlinearity, Pc has a host of other properties that make it an attractive candidate for practical limiters. The molecule itself can

be readily modified by bonding one of more than seventy metal ions to its center or adding peripheral and axial substituents<sup>5</sup>. Such alterations can have a significant effect on the behavior of the molecule, changing solubility<sup>14</sup>, heating response<sup>2</sup>, optical absorbance<sup>12</sup>, and other characteristics, potentially allowing manufacturers to create filters suited to many different situations with only relatively minor changes to the synthesis process. Phthalocyanine is frequently studied in liquid media<sup>3,5,19,22,24,31</sup>, with many derivatives having good solubility in a wide range of solvents<sup>5,14</sup>. Nanoscale thin films are another common medium, and more suited to practical filters. Films can be fabricated via a number of methods, including spin coating<sup>7</sup>, molecular beam epitaxy<sup>8</sup>, the Langmuir-Blodgett procedure<sup>7</sup>, monolayer self-assembly<sup>7</sup>, and thermal evaporation, the method used in this study. Thin films of Pc show remarkable flexibility due to weak intermolecular bonding<sup>18</sup>, a widening of absorption bands compared to solutions<sup>11</sup>, and the ability to further tune the material's properties by altering fabrication parameters<sup>12,16</sup>.

Although the majority of optical studies of Pc use pulsed lasers<sup>3,5,8,11,19,21,22,25,26,27,31</sup>, the relatively few that use continuous wave (CW) lasers have generally, though not universally, found strong saturable absorption (SA) behavior, the material growing more transparent in response to increased irradiance<sup>23,24</sup>. While this would contraindicate Pc as material for laser safety lenses in situations where CW lasers are a risk, it raises the possibility of using Pc in a range of other applications in which SA is desirable, such as mode locking, pulse shaping, and light measuring techniques<sup>4</sup>.

Herein, we study the optical response of thin films of metal-free phthalocyanine  $(H_2Pc)$ , iron phthalocyanine (FePc), and zinc phthalocyanine (ZnPc) when exposed to a CW laser using a simplified open-aperture z-scan procedure. We also vary the deposition temperature of our  $H_2Pc$  films, a parameter known to affect crystalline size and structure  $^{13,17}$ , to determine its effect on nonlinear absorption. In addition to films, a solution of tetra-tert-butyl-phthalocyanine (TTBPc) in chloroform was also measured using the z-scan method. We find evidence of strong saturable absorption in our thin films, with significant dependence on the metal complex used and no significant correlation between deposition temperature and nonlinear absorption. We observe a SA-to-RSA transition at high irradiances in our TTBPc-in-chloroform sample.

## 2. Experiment

The liquid sample consists of  $9.8 \times 10^{-6} \,\mathrm{M}$  TTBPc in chloroform. TTBPc powder of 97% purity was acquired from Sigma-Aldrich and dissolved in chloroform until the desired concentration was reached. The solution was placed in a 1 mm thick quartz cuvette for measurement.

Similarly, powders of  $H_2Pc$ , FePc, and ZnPc were acquired from Sigma Aldrich. The powders were outgased in-situ for several hours before thermal evaporation in a high vacuum system with base pressure of around  $10^{-6}$  mbar. For each deposition, a

Table 1. The deposition temperature  $T_{\rm dep}$  refers to the 1 mm glass substrate temperature during deposition. The thickness l is obtained from an in-situ quartz crystal monitor. The linear absorption  $\alpha_0$  is measured at the laser's wavelength of 633 nm.

Material	$T_{\rm dep}$ (°C)	l (nm)	$(10^6 \text{m}^{-1})$
$H_2Pc$	25	63	30
$H_2Pc$	100	57	34
$H_2Pc$	150	58	35
$H_2Pc$	200	59	27
$H_2Pc$	250	58	31
ZnPc	100	64	27
FePc	100	55	20

1 mm glass substrate was carefully cleaned for vacuum evaporation. Each substrate was heated to a constant deposition temperature  $T_{\text{dep}}$ . It is known that the deposition temperature from room temperature to 250 °C gradually increases the molecular crystal sizes in the thin film $^{13}$ . The film thickness l was monitored with an in-situ quartz crystal monitor (QCM) to cap at 60 nm. A summary of the deposition parameters of each film can be found in Table 1. The linear optical absorption coefficient  $\alpha_0$  of each thin film sample was measured in a photospectrometer<sup>12</sup>, and extracted for  $\lambda = 633 \, \text{nm}$ , see Fig. 1.

A 633 nm CW HeNe laser (JDS Uniphase 1101) with maximum output power of 3.87 mW was focused to a spot with an experimentally observed radius of 10 µm to 17 µm, resulting in a maximum irradiance between 12 MW/m<sup>2</sup> and 4.3 MW/m<sup>2</sup>. The sample was mounted on a track straddling the beam waist. In all figures, z =0 mm is the location of the experimentally observed waist.

To quantify the nonlinear absorption of these samples, the nonlinear absorption (NLA) coefficient  $\beta$  is extracted from a fit of the data. In the absence of NLA, the irradiance  $I_T$  of light transmitted by a material with thickness l is governed by the Beer-Lambert law  $I_T = I_0 e^{-\alpha_0 l}$ , where  $I_0$  is the irradiance of light incident on the sample and  $\alpha_0$  is the linear absorption coefficient. When third-order nonlinear processes such as two-photon absorption are significant, the linear absorption coefficient becomes dependent on the incident irradiance, such that it can be expanded to

$$I_T = I_0 e^{-(\alpha_0 + \beta I_0)l} \tag{2.1}$$

The NLA coefficient  $\beta$  is negative when describing SA behavior, and positive when describing RSA behavior.

To extract  $\beta$ , a simplified open-aperture z-scan procedure, adapted from that described by Sheik-Bahae et al.<sup>29</sup>, was applied to the samples. Each sample was mounted on a horizontal track and shifted through the beam waist in 1 mm steps.

The optical power of the light transmitted by the sample was measured at each step. A separate measurement was performed with the sample removed to measure the power of light incident on the sample. The transmittance of the sample at each z-position was then computed by dividing incident power by transmitted power.

The transmittance was normalized by dividing transmittance at every z-position by the average far-field transmittance. As derived by Sheik-Bahae et al.<sup>29</sup>, normalized transmittance as a function of z-position  $T_N(z)$  for an open-aperture z-scan is given by

$$T_N(z) = \sum_{m=0}^{\infty} \left( \frac{-q_0}{1 + ((z - p_o)/z_0)^2} \right)^m \cdot \frac{1}{(m+1)^{3/2}}$$
 (2.2)

Here,  $z_0$  is the Rayleigh diffraction length, itself given by

$$z_0 = n\pi w_0^2 / \lambda \tag{2.3}$$

Where n is the index of refraction of the propagation medium, approximated as 1,  $w_0$  is the beam radius at the waist, and  $\lambda$  is the wavelength of the laser, 633 nm. The Rayleigh diffraction length  $z_0$  is considered a free parameter, found via a numeric fit of the data. It is used to estimate the waist radius, which may slightly vary from sample-to-sample due to nonlinear refractive effects.

The peak position  $p_o$  is the z-position of the transmittance peak, and is another free parameter. The third free parameter is the q-factor  $q_0$ , defined as

$$q_0 = \beta I_0 L_{\text{eff}},\tag{2.4}$$

where  $L_{\text{eff}} = (1 - e^{-\alpha_0 l})/\alpha_0$  is the effective length of the sample and l is the thickness of the sample.

The values of l and  $\alpha_0$  depend upon the sample and are listed in Table 1. The waist radius  $w_0$  was extracted from the fit value of  $z_0$ , and the maximum irradiance was found by dividing the output power of 3.87 mW by the cross-sectional area of the beam assuming a radius of  $w_0$ . The first seven terms of the sum in Eq. 2.2 are sufficient to obtain results with more than three significant digits.

### 3. Results

The linear absorption coefficient as a function of irradiation wavelength for the thin films under study are shown in Fig. 1. The normalized transmittance as a function of z-position for samples of  $\rm H_2Pc$ ,  $\rm ZnPc$ , and  $\rm FePc$  deposited at 100 °C with approximately equal thickness is compared in Fig. 2. Their respective fit parameters and extracted values can be found in Table 2. The significantly lower linear absorption in FePc and ZnPc results from the addition of metal complexes,

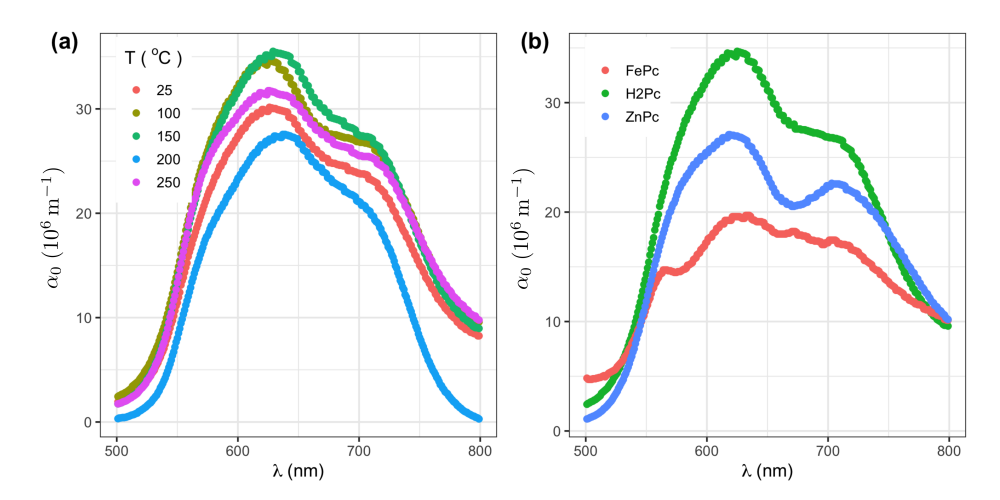


Figure 1. Absorption spectra (a) for H<sub>2</sub>Pc thin films deposited from room temperature to 250 °C, and (b) for FePc, H<sub>2</sub>Pc, and ZnPc deposited at 100 °C. Data from T. Fry<sup>12</sup>.

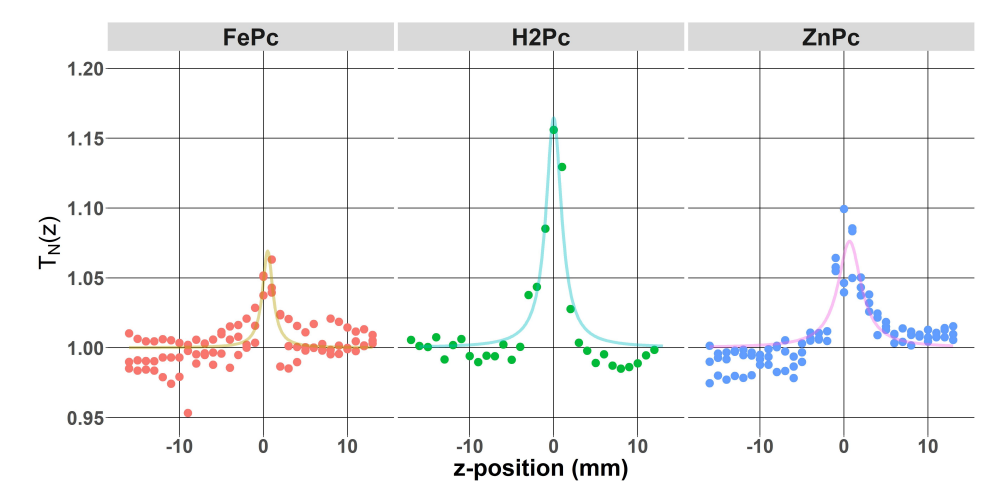


Figure 2. Normalized transmittance  $T_N$  vs z-position of H<sub>2</sub>Pc, FePc, and ZnPc thin films. Lines

which generally decreases the extinction coefficient of the phthalocyanine molecule by altering molecular energy levels<sup>8</sup>.

All samples exhibit strong saturable absorption. The nonlinear coefficient of the  $H_2Pc$  sample was calculated to be  $4.5\times$  larger than that of FePc, and  $1.7\times$  that of ZnPc (see Table 2). Given the similar thicknesses and deposition temperatures - and thus crystallite sizes - of the samples, it is suggested this difference in nonlinearity is due to the metal complexes themselves. The difference in Rayleigh diffraction length - and associated beam waist radius - between the samples is surmised to be

Table 2. Fit parameters  $(q_0 \text{ and } z_0)$  and extracted values for each thin film deposited at 100 °C. See Table 1 for the thickness and absorption coefficient of the samples, used to compute  $L_{\rm eff}$ .

Material	$q_0$	$z_0 \pmod{mm}$	w <sub>0</sub> (μm)	$I_0$ (MW/m <sup>2</sup> )	$L_{\text{eff}}$ (nm)	β (m/W)
$\mathrm{H_{2}Pc}$	-0.368	1.27	16.0	4.80	25.0	-3.06
FePc	-0.177	0.78	12.5	7.83	33.6	-0.67
ZnPc	-0.193	1.78	19.2	3.43	30.9	-1.82

due to uncertainty in the fit. It is also possible that this is due in part to nonlinear refractive effects such as thermal lensing causing the beam focus to change. Since SA effects are frequently attributed to depopulation of the ground state when pumping time is long compared to relaxation times  $^{33}$  - as is the case for CW irradiation - this is likely related to differences in linear absorption, with  $\rm H_2Pc$  having the highest  $\alpha_0$  and FePc the lowest.

The normalized transmittances as a function of z-position for samples of  $\rm H_2Pc$  deposited at 25 °C, 100 °C, 150 °C, 200 °C, and 250 °C are compared in Fig. 3. The fit parameters and extracted values can be found in Table 3.

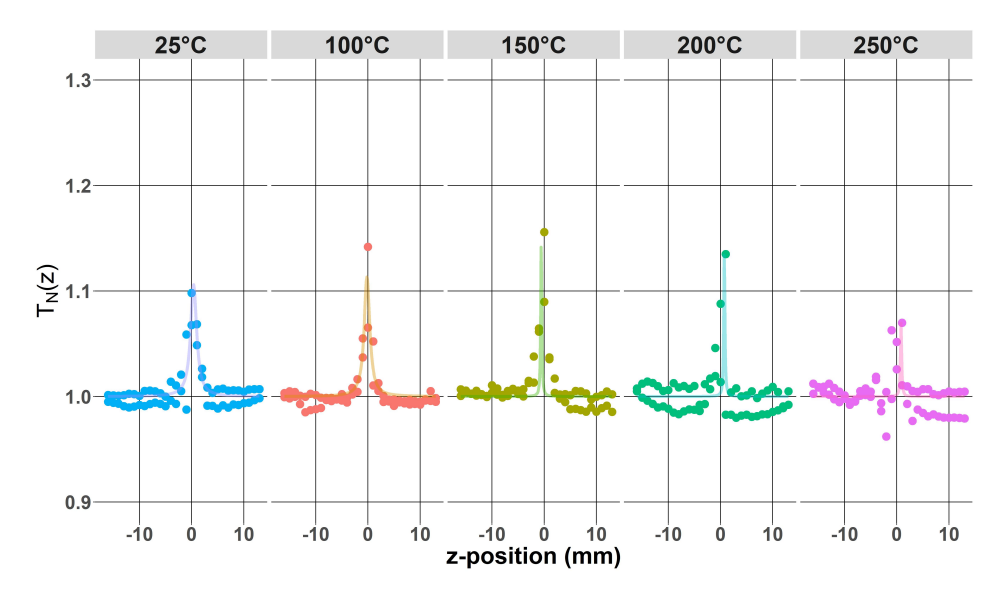


Figure 3. Normalized transmittance  $T_N$  vs z-position of H<sub>2</sub>Pc thin films deposited at 25 °C, 100 °C, 150 °C, 200 °C, and 250 °C. Lines are fits to data.

The magnitude of  $\beta$  appears to generally decline with increasing deposition temperature, with a large decrease between the sample fabricated at 100 °C and the sample fabricated at 150 °C. However, this may be caused in part by the large increase in apparent waist irradiance between these two samples. This increase is

Table 3. Fit parameters  $(q_0 \text{ and } z_0)$  for  $H_2Pc$  thin films with different deposition temperatures  $T_{\rm dep}$ . See Table 1 for the thickness and absorption coefficient of the same samples, used to compute  $L_{\text{eff}}$ .

$T_{\text{dep}}$ (°C)	$q_0$	$z_0 \pmod{mm}$	w <sub>0</sub> (μm)	$I_0$ (MW/m <sup>2</sup> )	$L_{\text{eff}}$ (nm)	β (m/W)
25	-0.257	0.759	12.4	8.06	28.4	-1.12
100	-0.272	0.700	11.9	8.73	25.0	-1.24
150	-0.331	0.124	5.0	49.3	24.7	-0.29
200	-0.331	0.134	5.2	45.7	29.3	-0.25
250	-0.177	0.134	5.2	45.6	26.7	-0.15

thought to be due to uncertainty in the fit because of low scan resolution about the beam waist rather than an actual increase in irradiance. Additionally, damage and imperfection in the samples might result in local thickness variations that introduce additional uncertainty in the values of the extracted parameters. The relatively small variation in  $\beta$  among the first two samples and among the last three indicates that if a relationship does exist between deposition temperature and nonlinear absorption, it is only weak.

The presence of strong SA contrasts with the RSA behavior has been previously observed in pulsed laser studies of metal phthalocyanines<sup>3,25,27,31,11,19</sup>. Since the laser wavelength falls near a linear absorption maximum, it is expected that the material is more likely to exhibit SA <sup>30,9</sup>. The duration of pumping is also expected to play a role in the direction of nonlinearity. RSA in phthalocyanine is reported to be governed by excited state absorption (ESA) and two photon absorption (TPA)<sup>34</sup>. When phthalocyanine is exposed to pulsed radiation, ESA is a primarily fluence-dependent process with little dependence upon pulse width. TPA, however, is strongly dependent upon pulse width, with increased width resulting in decreased RSA behavior both theoretically and experimentally.<sup>34</sup> In the limit of infinite width, e.g. a CW laser, the RSA behavior is expected to be much weaker than under nanosecond pulsed irradiation, allowing SA processes to dominate.

Normalized transmittance as a function of z-position for the TTBPc-inchloroform sample is shown in Fig. 4. A range of 41 z-positions is presented to demonstrate the presence of SA at all sample positions, even far from the beam waist. The "far-field" was taken to be z = -20, -19, 19, and 20 mm in these plots. A fit of measurements in the RSA region, between z = -5 and z = 5 mm, using Eq. 2.2 is also shown in Fig. 4. Data from each of the three runs were renormalized with a scale factor taken to be the average of the normalized transmittances at z=-5, -4, 4, and 5 mm for the purposes of this fit. A single fit was then created using renormalized data from all three runs and then multiplied by the scale factor before plotting.

The TTBPc sample exhibits a very broad peak about the waist, with a sudden and dramatic dip within a few millimeters of the actual waist position.

A sample of pure chloroform in the same cuvette was measured, and the response was found to be highly linear. Similar SA to RSA transitions have been reported previously; for example, Rao et al. reported such a transition during a study of alkyl-phthalocyanine nanoparticles in chloroform solution<sup>26</sup>. Vivas et al. similarly observed a transition in a z-scan study of lutetium bisphthalocyanine in chloroform<sup>33</sup>. SA to RSA transitions in phthalocyanines are typically identified with pump wavelengths around the Q-band of the absorption spectrum<sup>32</sup>. In bisphthalocyanine, this has been explained through a dramatic decrease in the ground state absorption cross section and a simultaneous increase in the excited state cross section at the edges of the Q-band using a three-level model<sup>33</sup>.

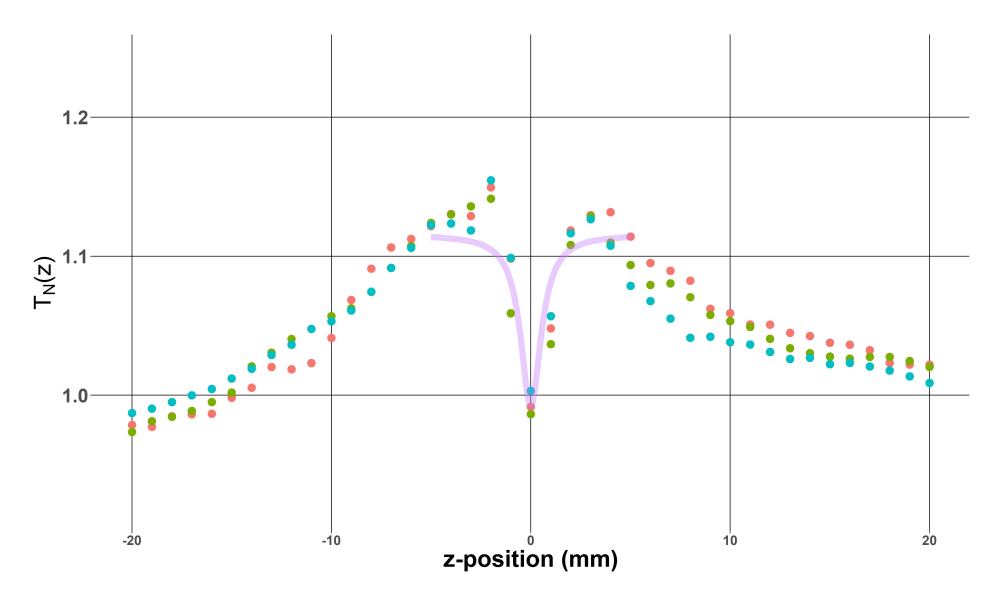


Figure 4. Normalized transmittance  $T_N$  vs z-position of TTBPc in chloroform. The three runs, marked in different colors, were performed in sequence over a period of several hours.

To permit a rough estimate of the NLA coefficient about the beam waist, we use an approximated linear absorption coefficient  $\alpha_0^*$  for a related phthalocyanine derivative, 1,8,15,22-tetraalkoxy-phthalocyanine (hereafter referred to as TAPc). The molar attenuation coefficient  $\epsilon$  for TAPc was measured by Apostol et al.<sup>2</sup> using a  $5 \times 10^{-6}$  M solution of TAPc in chloroform. From their absorption spectrum plot, we estimate  $\epsilon$  to be  $31\,500\,\mathrm{M}^{-1}\mathrm{cm}^{-1}$  at  $633\,\mathrm{nm}$ , and thus  $\alpha_0^*$  for the TTBPc sample was estimated to be  $31\,\mathrm{m}^{-1}$ . With this value we approximate the effective length  $L_{\mathrm{eff}}^*$  of our sample to be 0.985 mm.

The fit of the three runs using Eq. 2.2 and assuming a waist at z=0 returned a value of  $0.38\pm0.06$  for  $q_0$  and  $0.56\pm0.16$  for  $z_0$ . The apparent waist irradiance across the three runs is thus  $11\pm4$  MW/m<sup>2</sup>, and the approximated NLA coefficient  $\beta^*$  is 3.6  $\pm$  1.4  $\times$  10<sup>-5</sup> m/W. Apparent waist irradiance could be higher than that estimated

Table 4. Two photon absorption coefficient  $\beta$  and experimental parameters for selected studies (Ref.) of saturable absorbers as thin films (TF) with thickness l under continuous wave (CW) laser pumping.

Material	Medium	Pulse Length	l	β	Ref.
		(ns)	$(\mu m)$	(m/W)	
OHPc	1% in PMMA TF	CW	10	$-6.1 \times 10^{-4}$	23
ZnOHPc	1% in PMMA TF	$^{\mathrm{CW}}$	10	$-6.8 \times 10^{-4}$	23
ZnTriTBPc	1% in PMMA TF	$^{\mathrm{CW}}$	10	$-9.1 \times 10^{-3}$	23
TTBPc	1% in PMMA TF	$^{\mathrm{CW}}$	9	$-4.9 \times 10^{-3}$	24
ZnTTBPc	1% in PMMA TF	$^{\mathrm{CW}}$	12	$-1.1 \times 10^{-2}$	24
Mn-Doped ZnO	Doped with 1% Mn	$^{\mathrm{CW}}$	0	$-1.2 \times 10^{-1}$	1
CuPc nanoparticles	$\operatorname{TF}$	$8.0 \times 10^{-5}$	1	$-5.3 \times 10^{-3}$	35
Amido Black 10B	$4 \times 10^{-4} \mathrm{M}$ in PVA TF	$^{\mathrm{CW}}$	85	$-3.5 \times 10^{-4}$	30
ZnPc	TF	$2.5 \times 10^{-4}$	0.2	$-3.5 \times 10^{-9}$	20
BG dye	$0.05\mathrm{mM}$ in water	$^{\mathrm{CW}}$	$10^{3}$	$2.1 \times 10^{-5}$	6
CeO <sub>2</sub> -CoPc	0.1% in water	$^{\mathrm{CW}}$	-	$6.9 \times 10^{-5}$	28
TTBPc	$5\times 10^{-4}\mathrm{M}$ in $\mathrm{CHCl}_3$	6	$10^{3}$	$3.1 \times 10^{-9}$	19

for our thin films due to greater fit uncertainty related to the use of significantly fewer data points. Our estimates for  $\beta^*$  indicate weak RSA behavior about the beam waist, although our values are greater by four to five orders of magnitude than those reported in pulsed-laser studies of TTBPc-in-chloroform solution <sup>19</sup> and related phthalocyanines in other solvents<sup>25,3</sup>. It should be noted however that, due to the use of the linear absorption of TAPc rather than TTBPc,  $\beta^*$  is only an approximation of the actual NLA coefficient  $\beta$ .

The two-photon coefficients and relevant experimental parameters of other SA and RSA materials are listed in Tab. 4. The measured  $\beta$  values from Tab. 3 are much larger, sometimes exceeding these coefficients by two orders of magnitude or more. This may be due to the relatively high molecular density in thin films compared to the low-concentration solutions and doped thin films. Moreover, the relatively large beam cross-section impinging on the detector exaggerates the effects of refraction in the present measurements. It should be noted that there have been few studies of the archetype phthalocyanine thin films using CW irradiation to date, limiting a comparison.

## 4. Conclusion

All thin film samples of H<sub>2</sub>Pc, FePc, and ZnPc were observed to act as strong SAs, with H<sub>2</sub>Pc exhibiting the greatest nonlinearity, followed by ZnPc and FePc. No significant correlation was observed between deposition temperature and nonlinear absorption, although noise and low scan resolution introduce significant uncertainty into our measurements of  $\beta$ . This appears to contraindicate H<sub>2</sub>Pc, FePc, and ZnPc thin films for use as practical optical limiters in situations where CW lasers might be encountered, but their strong SA behavior recommends them for applications in which SA is desirable. TTBPc dissolved in chloroform appears to act as a SA at irradiances as low as  $4 \,\mathrm{kW/m^2}$ , but acts as an RSA at irradiances around  $4 \,\mathrm{MW/m^2}$  to  $12 \,\mathrm{MW/m^2}$ .

## 5. Acknowledgements

Thin film samples were fabricated via thermal evaporation by Taylor Fry as described elsewhere<sup>12</sup>. Dr. Hadi Tavassol assisted with the chloroform aspect of sample preparation. The work is partially supported by the National Science Foundation under Grant No. 2018653.

### References

- M. Abd-Lefdil, A. Belayachi, S. Pramodini, P. Poornesh, A. Wojciechowski and A. O. Fedorchuk, Structural, photoinduced optical effects and third-order nonlinear optical studies on Mn doped and Mn–Al codoped ZnO thin films under continuous wave laser irradiation, Laser Physics 24 (February 2014) p. 035404.
- P. Apostol, A. Bentaleb, M. Rajaoarivelo, R. Clérac and H. Bock, Regiospecific synthesis of tetrasubstituted phthalocyanines and their liquid crystalline order, *Dalton Transactions* 44 (March 2015) 5569–5576.
- O. M. Bankole, Y. Yılmaz and T. Nyokong, Nonlinear optical behavior of alkyne terminated phthalocyanines in solution and when embedded in polysulfone as thin films: Effects of aggregation, Optical Materials 51 (January 2016) 194–202.
- 4. W. Blau, H. Byrne, W. M. Dennis and J. M. Kelly, Reverse saturable absorption in tetraphenylporphyrins, *Optics Communications* **56** (November 1985) 25–29.
- 5. M. Calvete, G. Y. Yang and M. Hanack, Porphyrins and phthalocyanines as materials for optical limiting, *Synthetic Metals* **141** (March 2004) 231–243.
- R. K. Choubey, S. Medhekar, R. Kumar, S. Mukherjee and S. Kumar, Study of nonlinear optical properties of organic dye by Z-scan technique using He-Ne laser, Journal of Materials Science: Materials in Electronics 25 (March 2014) 1410-1415.
- 7. M. J. Cook, Thin film formulations of substituted phthalocyanines, *Journal of Materials Chemistry* **6** (January 1996) 677–689.
- G. de la Torre, P. Vázquez, F. Agulló-López and T. Torres, Role of Structural Factors in the Nonlinear Optical Properties of Phthalocyanines and Related Compounds, Chemical Reviews 104 (September 2004) 3723–3750.
- X. Deng, X. Zhang, Y. Wang, Y. Song, S. Liu and C. Li, Intensity threshold in the conversion from reverse saturable absorption to saturable absorption and its application in optical limiting, *Optics Communications* 168 (September 1999) 207– 212.
- S.-J. Ding, F. Nan, D.-J. Yang, X.-L. Liu, Y.-L. Wang, L. Zhou, Z.-H. Hao and Q.-Q. Wang, Largely Enhanced Saturable Absorption of a Complex of Plasmonic and Molecular-Like Au Nanocrystals, Scientific Reports 5 (April 2015) p. 9735.
- D. Dini, M. Barthel and M. Hanack, Phthalocyanines as Active Materials for Optical Limiting, European Journal of Organic Chemistry 2001(20) (2001) 3759–3769.
- T. D. Fry, Metallophthalocyanine Optical Properties Dependence on Grain Size, M.S. Thesis, California State University, Long Beach, (United States – California, 2018).
- K. P. Gentry, T. Gredig and I. K. Schuller, Asymmetric grain distribution in phthalocyanine thin films, *Physical Review B* 80 (November 2009) p. 174118.
- F. Ghani, J. Kristen and H. Riegler, Solubility Properties of Unsubstituted Metal Phthalocyanines in Different Types of Solvents, *Journal of Chemical & Engineering* Data 57 (February 2012) 439–449.

- 15. D. Gounden, N. Nombona and W. E. van Zyl, Recent advances in phthalocyanines for chemical sensor, non-linear optics (NLO) and energy storage applications, Coordination Chemistry Reviews 420 (October 2020).
- 16. T. Gredig, C. N. Colesniuc, S. A. Crooker and I. K. Schuller, Substrate-controlled ferromagnetism in iron phthalocyanine films due to one-dimensional iron chains, Physical Review B 86 (July 2012) p. 014409.
- 17. T. Gredig, E. A. Silverstein and M. P. Byrne, Height-Height Correlation Function to Determine Grain Size in Iron Phthalocyanine Thin Films, Journal of Physics: Conference Series 417 (March 2013) p. 012069.
- 18. Y. Han, W. Ning, H. Du, J. Yang, N. Wang, L. Cao, F. Li, F. Zhang, F. Xu and M. Tian, Preparation, optical and electrical properties of PTCDA nanostructures, Nanoscale 7 (October 2015) 17116–17121.
- 19. R. S. S. Kumar, S. V. Rao, L. Giribabu and D. N. Rao, Femtosecond and nanosecond nonlinear optical properties of alkyl phthalocyanines studied using Z-Scan technique, Chemical Physics Letters 447 (October 2007) 274-278.
- 20. S. Kumar, K. V. Anil Kumar, S. M. Dharmaprakash and R. Das, Phase-dependent ultrafast third-order optical nonlinearities in metallophthalocyanine thin films, Journal of Applied Physics 120 (September 2016) p. 123104.
- 21. M. C. Larciprete, R. Ostuni, A. Belardini, M. Alonzo, G. Leahu, E. Fazio, C. Sibilia and M. Bertolotti, Nonlinear optical absorption of zinc-phthalocyanines in polymeric matrix, Photonics and Nanostructures - Fundamentals and Applications 5 (October 2007) 73–78.
- F. Li, Z. He, M. Li and P. Lu, Three-photon absorption of copper phthalocyanine solution by femtosecond Z-Scan technique, Materials Letters 111 (November 2013)
- S. J. Mathews, S. Chaitanya Kumar, L. Giribabu and S. Venugopal Rao, Large third-order optical nonlinearity and optical limiting in symmetric and unsymmetrical phthalocyanines studied using Z-Scan, Optics Communications 280 (December 2007) 206-212.
- 24. S. J. Mathews, S. C. Kumar, L. Giribabu and S. V. Rao, Nonlinear optical and optical limiting properties of phthalocyanines in solution and thin films of PMMA at 633 nm studied using a cw laser, Materials Letters 61 (September 2007) 4426–4431.
- 25. G. N. Ngubeni, J. Britton, J. Mack, E. New, I. Hancox, M. Walker, T. Nyokong, T. S. Jones and S. Khene, Spectroscopic and nonlinear optical properties of the four positional isomers of  $4\alpha$ -(4-Tert-Butylphenoxy)Phthalocyanine, Journal of Materials Chemistry C 3 (October 2015) 10705–10714.
- 26. S. V. Rao, N. Venkatram, L. Giribabu and D. N. Rao, Ultrafast nonlinear optical properties of alkyl-phthalocyanine nanoparticles investigated using Z-Scan technique. Journal of Applied Physics 105 (March 2009) p. 053109.
- 27. S. V. Rao, P. T. Anusha, T. S. Prashant, D. Swain and S. P. Tewari, Ultrafast Nonlinear Optical and Optical Limiting Properties of Phthalocyanine Thin Films Studied Using Z-Scan, Materials Sciences and Applications 2 (May 2011) 299–306.
- 28. R. Sebastian and S. Sankararaman, Phthalocyanine-Induced Optical Nonlinearity in Ceria: A Z-Scan Study, Brazilian Journal of Physics 51 (August 2021) 1191–1198.
- 29. M. Sheik-Bahae, A. Said, T.-H. Wei, D. Hagan and E. Van Stryland, Sensitive measurement of optical nonlinearities using a single beam, IEEE Journal of Quantum Electronics **26** (April 1990) 760–769.
- G. Sreekumar, P. G. L. Frobel, C. I. Muneera, K. Sathiyamoorthy, C. Vijayan and C. Mukherjee, Saturable and reverse saturable absorption and nonlinear refraction in nanoclustered Amido Black dye-polymer films under low power continuous wave

- He–Ne laser light excitation, Journal of Optics A: Pure and Applied Optics 11 (September 2009) p. 125204.
- S. Tekin, U. Kürüm, M. Durmuş, H. G. Yaglioglu, T. Nyokong and A. Elmali, Optical limiting properties of zinc phthalocyanines in solution and solid PMMA composite films, Optics Communications 283 (December 2010) 4749–4753.
- 32. V. Viswanath, G. Subodh and C. I. Muneera, Zinc Phthalocyanine-Poly (Vinyl Alcohol) nanocomposite films: Low threshold optical limiting properties based on third-order nonlinear absorption response, *Optics & Laser Technology* **127** (July 2020) p. 106168.
- M. G. Vivas, E. G. R. Fernandes, M. L. Rodríguez-Méndez and C. R. Mendonca, Study
  of singlet excited state absorption spectrum of lutetium bisphthalocyanine using the
  femtosecond Z-Scan technique, *Chemical Physics Letters* 531 (April 2012) 173–176.
- 34. T.-H. Wei, T.-H. Huang and T.-C. Wen, Mechanism of reverse saturable absorption in chloro-aluminum phthalocyanine solution studied with Z-scan, *Chemical Physics Letters* **314** (December 1999) 403–410.
- S. Zongo, M. S. Dhlamini, P. H. Neethling, A. Yao, M. Maaza and B. Sahraoui, Synthesis, characterization and femtosecond nonlinear saturable absorption behavior of copper phthalocyanine nanocrystals doped-PMMA polymer thin films, *Optical Materials* 50 (December 2015) 138–143.